Acta Astronautica 126 (2016) 275–285

Contents lists available at ScienceDirect

Acta Astronautica

journal homepage: www.elsevier.com/locate/aa

Optimal low-thrust spiral trajectories using Lyapunov-based guidance

Da-lin Yang [a,*], Bo Xu [b], Lei Zhang [c]

[a] Shanghai Institute of Satellite Engineering, China
[b] School of Astronomy and Space Science, Nanjing University, China
[c] Satellite Communication and Navigation Collaborative Innovation Center, China

ARTICLE INFO

Article history:
Received 11 January 2016
Accepted 27 April 2016
Available online 5 May 2016

ABSTRACT

For an increasing number of electric propulsion systems used for real missions, it is very important to design optimal low-thrust spiral trajectories for these missions. However, it is particularly challenging to search for optimal low-thrust transfers. This paper describes an efficient optimal guidance scheme for the design of time-optimal and time-fixed fuel-optimal low-thrust spiral trajectories. The time-optimal solution is obtained with Lyapunov-based guidance, in which the artificial neural network (ANN) is adopted to implement control gains steering and the evolutionary algorithm is used as the learning algorithm for ANN. Moreover, the relative efficiency introduced in Q-law is analyzed and a periapis-and-apoapsis-centered burn structure is proposed for solving time-fixed fuel-optimal low-thrust orbit transfer problem. In this guidance scheme, the ANN is adopted to determine the burn structure within each orbital revolution and the optimal low-thrust orbit transfer problem is converted to the parameter optimization problem. This guidance scheme runs without an initial guess and provides closed form solutions. In addition, Earth J2 perturbation and Earth-shadow eclipse effects are considered in this paper. Finally, a comparison with solutions given by the literature demonstrates the effectiveness of the proposed method.

1. Introduction

The implementation of electric propulsion (EP) system on Earth-orbit satellites, especially for geostationary satellites, has been a preferred option due to the much higher specific impulse of EP systems. Consequently, it is increasingly important to be able to design optimal transfer trajectories for these missions. However, the optimization of Earth-orbit transfers with EP system is still a challenging problem. This is because the low control authority of the EP system as well as the existence of long powered arcs and subsequent hundreds or even thousands of orbital revolutions. Historically, the problem of computing low-thrust transfer trajectories has been studied extensively in the literatures [1,2]. Much of the work has concentrated on finding optimal transfer trajectories using either indirect or direct methods [3–10]. However, it is time consuming and tedious to obtain optimum solutions, and on the other hand the obtained solutions don't have the closed form. Meanwhile, some attentions have also been focused on using heuristic control law to achieve low-thrust orbit transfers [11,12]. The heuristic control law has the advantages of simple formulation and fast calculating speed, while the drawback lies in that the obtained solutions are usually not optimal.

Lyapunov-based guidance is a widely used heuristic method for computing low-thrust transfer trajectories where the candidate Lyapunov function must be defined by orbit designer. Ilgen [13] employed Kepler orbital elements in the Lyapunov function and developed a Lyapunov-based guidance for low-thrust orbit transfers. Chang [14] suggested a Lyapunov function based on angular momentum and eccentricity vectors and solved the low-thrust orbit transfer problem in Cartesian coordinates. Petropoulos [15,16] developed a candidate Lyapunov function based on analytic expressions for maximum rates of change of the orbital elements and introduced a mechanism for coasting based on the concept of relative efficiency. Yang [17] applied Lyapunov-based method to perform trade studies for the influence of space perturbation on low-thrust transfers. The disadvantage of the Lyapunov-based transfers mentioned above is that the obtained solutions are usually not optimal, basically because there is not a well-defined method to determine the gains in the Lyapunov-based guidance. Some researchers have started using stochastic algorithms to search the reasonable gains. Lee [18] investigated the parameter selection in a Lyapunov-based guidance by using evolutionary algorithm. Ren and Cui [19] investigated the problem of designing low-thrust transfers by using modified equinoctial elements and investigated the parameter selection in a Lyapunov-based

* Corresponding author.
E-mail addresses: yangdalin20088@126.com (D.-l. Yang), xubo@nju.edu.cn (B. Xu), zhangleiastro@gmail.com (L. Zhang).

http://dx.doi.org/10.1016/j.actaastro.2016.04.028
0094-5765/

guidance by using genetic algorithm. A comparison in Ref. [22] indicates that time-varying gains are more appropriate than constant gains in Lyapunov-based guidance. Gao [20,21] found that the Lyapunov-based guidance has a similar structure to the parameterized control law derived from the calculus of variations. Firstly, he used the Lyapunov-based transfer as an initial guess for direct optimization and obtained the optimal low-thrust transfer. Then, he investigated the problem of designing optimal low-thrust transfers by using a mapping between parameterized control law and the Lyapunov-based guidance law to determine time-varying gains in Lyapunov-based guidance. Yang [22] employed a smart Lyapunov-based method for minimum-time low-thrust orbit transfers, in which the artificial neural network (ANN) is adopted to implement gains steering and the evolutionary algorithm is used as the learning algorithm for ANN.

In this paper, we take advantage of Lyapunov stability theory to design guidance laws for minimum-time low-thrust orbit transfers as well as time-fixed minimum-propellant low-thrust orbit transfers. This involves constructing a suitable Lyapunov function that is always monotonic and minimum at the given target orbit. The method presented here is related to the method in Ref. [22], where the control gains time histories and the burn structure parameters are determined using ANN and the subsequent parameter optimization problem is solved using evolutionary algorithm. However, fuel-saving low-thrust transfer is not considered in Ref. [22]. The first problem solved in this paper is to design a closed-loop minimum-time guidance law for low-thrust orbit transfer, where no coast arc is considered in the transfer process except for the satellite in the Earth-shadow zone. The second problem solved in this paper is to design a closed-loop time-fixed minimum-propellant guidance law for low-thrust orbit transfer, where the relative thrust efficiency introduced in Ref. [16] is analyzed and a periapis-and-apoapsis-centered burn structure is proposed. The proposed burn structure is simple and its efficiency is high in the time-fixed minimum-propellant transfer trajectories computation. In addition, the employed evolutionary algorithm is also able to easily accommodate free variables in the minimum-propellant guidance law. What's more, an orbital averaging technique is used to quickly and efficiently compute low-thrust transfer trajectories in the presence of Earth-shadow eclipse and Earth J2 effects.

The primary objective of this paper is to propose an optimal closed form guidance law for low-thrust orbit transfer, which has strong ability of responding to perturbations. In Section 2, a brief description of low-thrust spiral trajectory optimization problem is given, including the dynamical model and orbital averaging technique. After a detailed description of the Lyapunov-based guidance in Section 3, both the minimum-time and time-fixed minimum-propellant spiral trajectories involving a periapis-and-apoapsis-centered burn structure are modeled and solved in Section 4. Two cases are presented and their results are analyzed in Section 5. At last, some conclusions are given in Section 6.

2. Problem statement

The optimization of low-thrust spiral trajectories is described using the modified equinoctial elements to circumvent the singularities caused by the use of Keplerian elements. The relationship between the modified equinoctial elements and the classical orbital elements are:

$$\begin{aligned} p &= a\left(1-e^2\right)\\ f &= e\ \cos(\omega+\Omega)\\ g &= e\ \sin(\omega+\Omega)\\ h &= \tan(i/2)\cos\ \Omega\\ k &= \tan(i/2)\sin\ \Omega\\ L &= \Omega+\omega+\upsilon \end{aligned} \tag{1}$$

where Ω is the longitude of ascending node, ω is the argument of perigee, and υ is the true anomaly. The equations of motion utilized a set of modified equinoctial elements [23], plus the appropriate rule for mass-flow rate which describe the motion of the EP satellite in an inverse-square gravity field are given by

$$\begin{aligned} \dot{p} &= \sqrt{\frac{p}{\mu}}\frac{2p}{w}f_t\\ \dot{f} &= \sqrt{\frac{p}{\mu}}\left\{f_r\ \sin\ L+[(1+w)\cos\ L+f]\frac{f_t}{w}-(h\ \sin\ L-k\ \cos\ L)\frac{g\cdot f_n}{w}\right\}\\ \dot{g} &= \sqrt{\frac{p}{\mu}}\left\{-f_r\ \cos\ L+[(1+w)\sin\ L+g]\frac{f_t}{w}+(h\ \sin\ L-k\ \cos\ L)\frac{f\cdot f_n}{w}\right\}\\ \dot{h} &= \sqrt{\frac{p}{\mu}}\frac{s^2 f_n}{2w}\ \cos\ L\\ \dot{k} &= \sqrt{\frac{p}{\mu}}\frac{s^2 f_n}{2w}\ \sin\ L\\ \dot{L} &= \sqrt{\mu p}\left(\frac{w}{p}\right)^2+\frac{1}{w}\sqrt{\frac{p}{\mu}}(h\ \sin\ L-k\ \cos\ L)f_n\\ \dot{m} &= -\frac{T}{g_0 I_{sp}} \end{aligned} \tag{2}$$

where $w=1+f\ \cos\ L+g\ \sin\ L$, $s^2=1+h^2+k^2$, μ is the gravitational constant of central body, T is the thrust magnitude, g_0 is the gravitational acceleration at the sea level, I_{sp} is the specific impulse. The terminal goal for the low-thrust spiral transfers is to determine the thrust acceleration components for minimum-time solution and time-fixed minimum-propellant solution. The thrust components in an orthogonal radial-horizontal (RSW) frame, where the unit vector R and S in orbital plane are along the local radial and transverse, and the unit vector W is along the angular momentum direction, can be expressed by:

$$\boldsymbol{u}=\frac{T}{m}\begin{bmatrix}\cos\ \alpha\ \cos\ \beta\\ \sin\ \alpha\ \cos\ \beta\\ \sin\ \beta\end{bmatrix} \tag{3}$$

where α is yaw angle and β is pitch angle, respectively. Our approach is to determine the thrust components based on Lyapunov stability theory and use evolutionary algorithm to optimize performance. The computation load is determined by the accurate numerical integration of the Eq. (2). Several works indicate that the computational load of orbit propagation is significantly reduced by using the orbital averaging technique [24].The fundamental principle of orbital averaging is that the “fast” equinoctial element L is defined by:

$$\frac{dL}{dt}\approx\sqrt{\mu p}\left(\frac{1+f\ \cos\ L+g\ \sin\ L}{p}\right)^2 \tag{4}$$

This is because that five equinoctial elements p, f, g, h and k vary slowly due to the small thrust components. Next the average time rate of change of the equinoctial elements p, f, g, h and k over an orbital period are defined by:

$$\begin{aligned} \dot{\bar{\boldsymbol{x}}} &= \frac{1}{P}\int_0^{2\pi}\frac{d\boldsymbol{x}}{dt}\frac{dt}{dL}dL\\ &= \frac{1}{2\pi}\left(1-\bar{f}^2-\bar{g}^2\right)^{3/2}\cdot\left[\int_{Lex}^{Len}\frac{\boldsymbol{f}_T}{w^2}dL+\int_0^{2\pi}\frac{\boldsymbol{f}_p}{w^2}dL\right] \end{aligned} \tag{5}$$

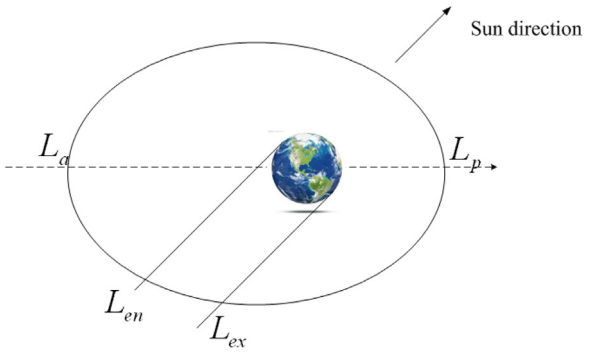

Fig. 1. Illustration of shadow zone within each revolution.

where $\bar{\boldsymbol{x}} = \left[\bar{p}\ \ \bar{f}\ \ \bar{g}\ \ \bar{h}\ \ \bar{k}\right]$ describes the mean equinoctial elements, P is the orbital period, $\boldsymbol{f}_T$ is the thrust acceleration components and $\boldsymbol{f}_p$ is the perturbation acceleration components. In this paper, a cylindrical shadow model is used to compute Earth-shadow entrance angle L_{en} and Earth-shadow exit angle L_{ex} (see Fig. 1), which are the limits of integration in Eq. (5). The power of the EP system is assumed to be zero when the satellite is in the Earth's shadow zone. Similarly, the averaged time rate of change of satellite mass over an orbital period can be defined by:

$$\frac{d\bar{m}}{dt} = \frac{1}{2\pi}\left(1 - \bar{f}^2 - \bar{g}^2\right)^{3/2} \cdot \int_{L_{ex}}^{L_{en}} \frac{\dot{m}}{w} dL \tag{6}$$

where $\bar{m}$ is the mean satellite mass. In this paper, the Gauss–Legendre quadrature method is applied to compute the approximate values of definite integrals in Eqs. (5) and (6). Because of the five equinoctial elements p, f, g, h and k vary slowly with time due to the thrust components. The low-thrust spiral transfer can be propagated ahead in time by using the large time steps on the order of several days. As a result, the computational burden can be reduced significantly.

3. Lyapunov-based guidance

Evaluating the performance of low-thrust transfer requires knowledge of thrust acceleration in the RSW orbital coordinate. In this paper, thrust-steering accelerations are derived by using the Lyapunov stability theory. The Lyapunov-based guidance presented here is related to that in Ref. [22]. The application of the Lyapunov-based guidance law begins by defining a candidate Lyapunov function for the optimal low-thrust transfer

$$V = \sum_{\xi} W_{\xi}\left(\frac{\xi - \xi_T}{\dot{\xi}_{\alpha,\beta,L}}\right)^2, \quad \text{for } \xi = p, f, g, h, k \tag{7}$$

where the five elements (ξ) are the modified equinoctial elements, (W_{ξ}) are control gains, the equinoctial element with the subscript T denotes the target value. The analytic expressions for the maximum time rate of change of modified equinoctial element $\dot{\xi}_{\alpha,\beta,L}$ are given in Ref. [22].

It is clear from the definition of the Lyapunov function in Eq. (7) that the functional value is zero at the target orbit and positive elsewhere. Thus, driving the satellite to the target orbit equals to reducing the functional value to zero. Once the expressions for $\dot{\xi}_{\alpha,\beta,L}$ are given, the Lyapunov function is only relative to the five orbit elements. Now, the time rate of change of Lyapunov function is given by

$$\frac{\mathrm{d}V}{\mathrm{d}t} = \sum_{\xi} \frac{\partial V}{\partial \xi}\dot{\xi} = (\partial V/\partial \boldsymbol{\xi})^T \dot{\boldsymbol{\xi}}$$

$$= (\partial V/\partial \boldsymbol{\xi})^T \boldsymbol{B}\frac{T}{m}\hat{\boldsymbol{u}} \tag{8}$$

where $\dot{\xi}$ can be obtained explicitly from the equations of motion in Eq. (2). Thus, unlike the Lyapunov function, the time rate of change of Lyapunov function is a function of the thrust angles. At any timing node in the process of transfer, the thrust angles make the time rate of change of Lyapunov function most negative are the minimum-time solutions for low-thrust spiral transfer.

$$\dot{V}_n = \min_{\alpha,\beta} \dot{V} \tag{9}$$

The direction $\hat{\boldsymbol{u}} = \left[\cos\alpha\cos\beta\ \ \sin\alpha\cos\beta\ \ \sin\beta\right]^T$ that minimizes the time rate of change of Lyapunov function can be obtained analytically

$$\hat{\boldsymbol{u}} = -\frac{\boldsymbol{B}^T(\partial V/\partial \boldsymbol{\xi})}{\|\boldsymbol{B}^T(\partial V/\partial \boldsymbol{\xi})\|} \tag{10}$$

Note that the time rate of change of Lyapunov function is always less zero, and the thrust direction in Eq. (10) ensure the maximum rate of reduction of Lyapunov functional value at the current true longitude. However, they do not provide any information about the effectivity of the thrust. It is well known that the efficiency is different at the different location on the osculating orbit. Thus, it is natural to define the relative effectivity of the thrust at the current true longitude [16].

$$\eta_r = \frac{\dot{V}_n - \dot{V}_{nx}}{\dot{V}_{nn} - \dot{V}_{nx}} \tag{11}$$

where

$$\dot{V}_{nn} = \min_{L} \dot{V}_n \tag{12}$$

$$\dot{V}_{nx} = \max_{L} \dot{V}_n \tag{13}$$

A mission designer can prevent the spacecraft from thrusting if the relative effectivity is below the given cut-off value. The larger the cut-off value, the more the expected propellant saving and the longer the expected flight time.

4. Optimal control problem formulation

The Lyapunov-based guidance described in the preceding section can realize the low-thrust spiral trajectory very well. The Lyapunov-based guidance has the advantages of simple formulation and quick calculating speed, while the drawback lies in that the obtained solutions are usually not optimal. This is because that a well-defined method is difficult to find to determine the gains or other free parameters in Lyapunov-based guidance. The remainder of this section will describe the minimum-time Lyapunov-based guidance scheme and the time-fixed minimum-propellant Lyapunov-based guidance scheme, as well as the application of them to search for optimal low-thrust spiral transfers.

4.1. Minimum-time transfer

The preceding section indicates that the thrust direction in Eq. (10) ensures the maximum rate of reduction of Lyapunov functional value at the current true longitude. In minimum-time guidance scheme, cut-off value is set to zero, which means that the thrust is applied continuously. The thrust direction equivalent to the pitch angle α and yaw angle β are available analytically.

However, numerical simulation results show that the performance of low-thrust spiral trajectory is sensitive to the gains in Lyapunov-based guidance law. As stated above, time-varying gains are more appropriate than constant gains in Lyapunov-based guidance law. For the minimum-time transfer, the design parameters are the time histories of the gains in Lyapunov-based guidance law. In this section, a novel gains steering strategy based on the perspective of artificial neural network and evolutionary algorithm is described.

From the statement, a minimum-time spiral trajectory can be regarded as the result of a Lyapunov-based gains steering strategy S: $\Upsilon \mapsto U$ that maps the satellite-relevant variables $\boldsymbol{X} \in \Upsilon$ to the gains $\boldsymbol{W}_\xi \in U$ in Lyapunov-based guidance.

$$S: \{\boldsymbol{\xi} \quad \boldsymbol{\xi}_T \quad m\} \in \Upsilon \mapsto \{\boldsymbol{W}_\xi\} \in U \tag{14}$$

where $\boldsymbol{\xi}$ are the osculating equinoctial elements, the variable with the subscript T denotes the target value, and m is the osculating satellite mass. The minimum-time transfer is the result of the optimal gains steering program S^*. Here, an ANN is used as a so-called gains steering to implement time-varying gains steering program. Consequently, the problem of searching for a minimum-time transfer is equivalent to the problem of searching for an optimal time-varying gains steering program S^*, in other words, searching for a set of optimal weights in ANN [25].

A feedforward network structure is applied to implement time-varying gains steering program, the detailed network structure including the input and output is described in Ref. [22]. In the proposed method, an improved cooperative evolutionary algorithm (ICEA) which works on a population through sharing the current optimal position of Particle Swarm Optimization (PSO) and Differential Evolution(DE) is applied to determine the optimal parameters $\boldsymbol{\pi}^*$ within ANN. The detailed updating process of ICEA is given in Ref. [26].

The optimality of a minimum-time transfer should be defined with respect to the transfer time. When the Lyapunov-based guidance law is used for trajectory optimization, the accuracy of the trajectory with respect to the terminal constraints must also be considered as a secondary optimization objective. Here, the transfer time for a geostationary orbit transfer using EP system is to be minimized. The performance index includes the transfer time and the final distance to the geostationary orbit. Since the target is the geostationary orbit, only three orbital elements need to be considered in terminal constraints. Besides, the terminal constraint with respect to each orbital element needs not to be satisfied exactly. Then, a maximal allowed error corresponding to each orbital element has to be defined. Using $\Delta a_{f\ \max}$, $\Delta e_{f\ \max}$ and $\Delta i_{f\ \max}$, the distances corresponding to semi-major axis a, eccentricity e and inclination i at the target can be normalized.

$$\Delta a_f = \frac{\left|a(t_f) - a_T\right|}{\Delta a_{f\ \max}} \tag{15}$$

$$\Delta e_f = \frac{\left|e(t_f) - e_T\right|}{\Delta e_{f\ \max}} \tag{16}$$

$$\Delta i_f = \frac{\left|i(t_f) - i_T\right|}{\Delta i_{f\ \max}} \tag{17}$$

Furthermore, a measure for the accuracy of the spiral transfer trajectory corresponding to the terminal constraints can be defined by

$$\Delta X_f = \sqrt{\frac{1}{3}\left((\Delta a_f)^2 + (\Delta e_f)^2 + (\Delta i_f)^2\right)} \tag{18}$$

Now, objective function may be defined with respect to the transfer time and the final distance to target orbit. It can be seen that the performance of Lyapunov-based guidance scheme depends strongly on their adequate composition. The primary sub-objective function corresponding to the transfer time is defined by

$$J_T = -1000\cdot\left(1 - \frac{t_f}{T_{\max}}\right) \tag{19}$$

where $T_{\max}$ is the maximal transfer time, and the sub-objective functions with respect to terminal constraints are defined by

$$J_a = \log_2\left(\frac{1}{\Delta a_f}\right)$$
$$J_e = \log_2\left(\frac{1}{\Delta e_f}\right)$$
$$J_i = \log_2\left(\frac{1}{\Delta i_f}\right) \tag{20}$$

If the requirements about terminal constraints are fulfilled, J_a, J_e and J_i are positive, and negative on the contrary. Numerical simulation results indicate that the search process should first concentrate on the terminal constraints requirement and then on the transfer time minimization. The full objective function for minimum-time transfers are modified by

$$J = \begin{cases} -\dfrac{1}{c_4 + (1-c_4)\sqrt{\left((\Delta a_f)^2 + (\Delta e_f)^2 + (\Delta i_f)^2\right)/3}} \\ \qquad \text{if } J_a < 0, J_e < 0, J_i < 0 \\ J_T - \dfrac{1}{c_4 + (1-c_4)\sqrt{\left((\Delta a_f)^2 + (\Delta e_f)^2 + (\Delta i_f)^2\right)/3}} \\ \qquad \text{if } J_a \geq 0, J_e \geq 0, J_i \geq 0 \end{cases} \tag{21}$$

The value for c_4 guarantees that once the requirement about terminal constraints is fulfilled, minimizing the transfer time has a higher priority than the improvements in the fulfillment of the terminal constraints. Here, $c_4 = 0.99$ is chosen.

In order to find a minimum-time transfer, the method proposed in this paper runs in two loops. The particular architecture sketched in Fig. 2 reflects its fundamental design principle to search for a minimum-time transfer. Within the trajectory integration loop, an ANN is applied to implement gains steering according to its network function that is completely defined by the ANN's weight set $\boldsymbol{\pi}$. The weight set $\boldsymbol{\pi}$ is adjusted and evaluated by the ICEA(improved cooperative evolutionary algorithm) [26] in the trajectory optimization loop. Within the trajectory optimization loop, the ICEA evaluates all ANN weight sets for their suitability to generate a minimum-time transfer. Within the trajectory integration loop, the ANN takes the osculating equinoctial elements $\boldsymbol{\xi}(t_i)$, the osculating satellite mass $m(t_i)$ and the target equinoctial

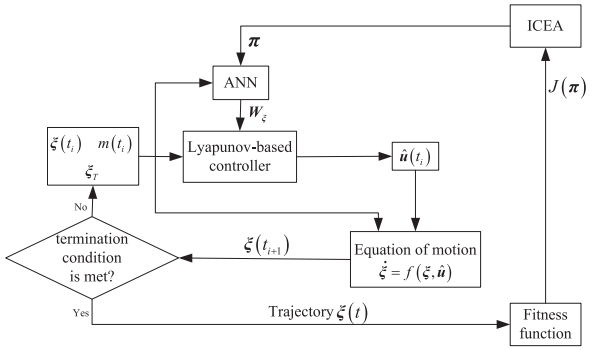

Fig. 2. The architecture of time-optimal scheme.

elements $\boldsymbol{\xi}_T$ as input values and maps them to the output values, from which the control gains can be derived. So the required thruster direction $\hat{\boldsymbol{u}}(t_i)$ can be calculated by using the Lyapunov-based guidance. The osculating equinoctial elements $\boldsymbol{\xi}(t_i)$, the osculating satellite mass $m(t_i)$ and the actual thrust program $\hat{\boldsymbol{u}}(t_i)$ are inserted into the equations of motion, which are numerically integrated over one step $\Delta t = t_{i+1} - t_i$ to yield $\boldsymbol{x}(t_{i+1})$. These equinoctial elements are fed back into the ANN until the termination condition is met. After that, the ANN's weight set is evaluated by the ICEA's fitness function $J(\boldsymbol{\pi})$, which is crucial for the probability of $\boldsymbol{\pi}$ to create optimal weight set $\boldsymbol{\pi}^*$. The ICEA converges against a single gains steering strategy, which adjusts the Lyapunov-based guidance to guide the spacecraft to fly along a minimum-time spiral trajectory $\boldsymbol{\xi}^*(t)$.

4.2. Time-fixed minimum-propellant transfer

The preceding section indicates that the efficiency of the thrust is different at the different location on the osculating orbit. The relative effectivity defined in Ref. [16] can make a well trade-off between the transfer time and the propellant consumption by varying the cut-off value of the relative efficiency. However, adjusting the cut-off value of the relative efficiency in time-fixed minimum-propellant transfer trajectory optimization requires large computational resources. The values for $\dot{V}_{nn}$ and $\dot{V}_{nx}$ are computed numerically, because analytic expressions for these are not available.

The variation of the relative efficiency with the increasing true anomaly is described in Fig. 3. It can be seen that the value of the relative efficiency reaches maximum when true anomaly is close to 180° (the apoapsis point on the osculating orbit). Besides, the effectivity value has a second extreme value when true anomaly is close to 0° or 360° (the periapsis point on the osculating orbit). In other words, the satellite is enabled for thrusting when it is near apogee or perigee on the osculating orbit. Consequently, the problem of searching for a time-fixed minimum-propellant transfer is equivalent to the problem of searching for an optimal periapis-and-apoapsis-centered burn structure (See Fig. 4).

The periapis-and-apoapsis-centered burn structure has the advantages of simple formulation and it is well involved into orbital averaging. The true longitude corresponding to the periapsis L_p and the apoapsis L_a are given by

$$\begin{aligned} L_p &= \omega + \Omega \\ L_a &= L_p + \pi \end{aligned} \tag{22}$$

Therefore, the periapis-and-apoapsis-centered burn structure

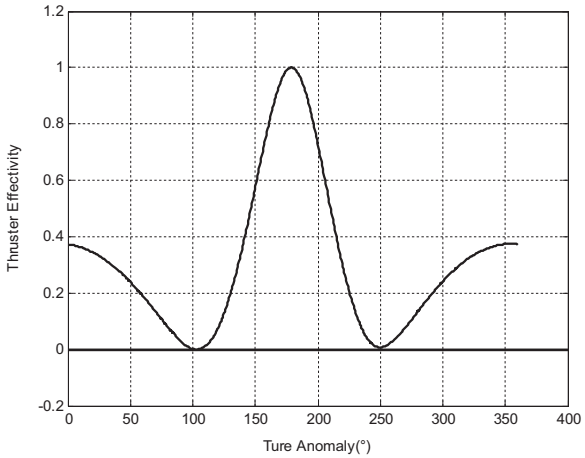

Fig. 3. The relationship between the relative effectivity and the true anomaly.

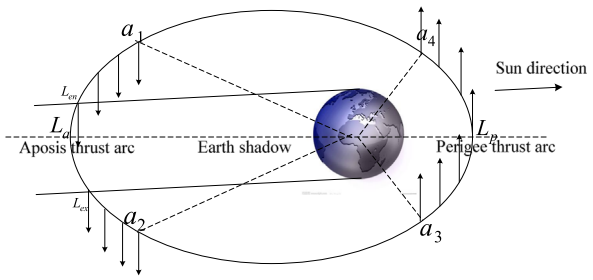

Fig. 4. The periapis-and-apoapsis-centered burn structure on the osculating orbit.

can be parameterized by using the variables like w_p and w_a

$$\begin{cases} a_1 = L_a - w_a\pi \\ a_2 = L_a + w_a\pi \end{cases} \quad (0 \le w_a \le 1)$$
$$\begin{cases} a_3 = L_p - w_p(1 - w_a)\pi \\ a_4 = L_p + w_p(1 - w_a)\pi \end{cases} \quad (0 \le w_p \le 1) \tag{23}$$

For the time-fixed minimum-propellant transfers, the integration range of orbital averaging tends to become discontinuous. For example, the integration limits for the orbital averaging integral in Fig. 5 are (a_1, L_{en}), (L_{ex}, a_2) and (a_3, a_4), respectively. In this case, the averaged time rates for the mean states due to thrust are computed by:

$$\dot{\bar{\boldsymbol{x}}} = \frac{1}{P}\int_0^{2\pi} \frac{d\boldsymbol{x}}{dt}\frac{dt}{dL}dL = \frac{1}{2\pi}\left(1 - \bar{f}^2 - \bar{g}^2\right)^{3/2} \cdot \left[\int_{a_1}^{Len} \frac{\boldsymbol{f}_T}{w^2}dL + \int_{L_{ex}}^{a_2} \frac{\boldsymbol{f}_T}{w^2}dL + \int_{a_3}^{a_4} \frac{\boldsymbol{f}_T}{w^2}dL + \int_0^{2\pi} \frac{\boldsymbol{f}_p}{w^2}dL\right] \tag{24}$$

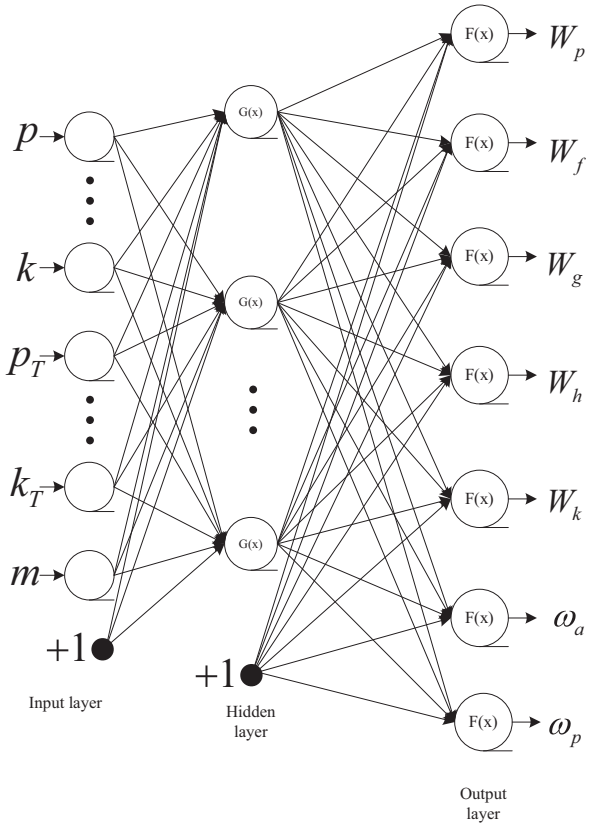

Fig. 5. Layered feedforward artificial neural network for time-fixed minimum-propellant transfer.

$$\frac{d\bar{m}}{dt}=\frac{1}{2\pi}\left(1-\bar{f}^2-\bar{g}^2\right)^{3/2}\cdot\left[\int_{a_1}^{Len}\frac{\dot{m}}{w}dL+\int_{L_{ex}}^{a_2}\frac{\dot{m}}{w}dL+\int_{a_3}^{a_4}\frac{\dot{m}}{w}dL\right] \tag{25}$$

Consequently, the design parameters for time-fixed minimum-propellant transfers are the time histories of the internal gains in Lyapunov-based guidance law and the time histories of the parameters for periapis-and-apoapsis-centered burn structure. A time-fixed minimum-propellant parameters steering strategy may be defined as an associative mapping S that maps the spacecraft-relevant variables $\boldsymbol{X}\in\Upsilon$ to the time-varying parameters $\left\{\boldsymbol{W}_\xi\ \ \omega_a\ \ \omega_p\right\}\in U$ in the time-fixed minimum-propellant Lyapunov-based guidance.

$$S:\left\{\boldsymbol{\xi}\ \ \boldsymbol{\xi}_T\ \ m\right\}\in\Upsilon\mapsto\left\{\boldsymbol{W}_\xi\ \ \omega_a\ \ \omega_p\right\}\in U \tag{26}$$

where $\boldsymbol{\xi}$ are the osculating equinoctial elements, the variable with the subscript T denotes the target value, and m is the osculating mass, $\boldsymbol{W}_\xi$ are the gains in Lyapunov-based guidance, ω_a and ω_p are the burn structure parameters. Consequently, the problem of searching for a time-fixed minimum-propellant transfer is equivalent to the problem of searching for an optimal time-varying parameters steering strategy S^*, in other words, searching optimal weights in ANN. In this paper, a feedforward network structure is applied to represent the optimal time-varying parameters steering strategy S^*. The neurons are organized in three layers: 12 neurons in the input layer, 20 neurons in hidden layer, and seven neurons in output layer (see Fig. 5). The neurons in the input layer accept osculating equinoctial elements, target equinoctial elements and osculating satellite mass as input, the input and the output corresponding to the neurons in input layer are given by

$$\begin{aligned}&\mathrm{In}^{(1)}(t)=\left[\boldsymbol{\xi}(t)\ \ \boldsymbol{\xi}^T\ \ m(t)\ \ +1\right]\\&\mathrm{Out}^{(1)}(t)=\mathrm{In}^{(1)}(t)\end{aligned} \tag{27}$$

Then the input and the output corresponding to the neurons in the hidden layer are given by

$$\begin{cases}\mathrm{In}_n^{(2)}(t)=\sum_{i=1}^{12}w_{ni}\cdot\mathrm{Out}_i^{(1)}(t)\\ \mathrm{Out}_n^{(2)}(t)=G(\mathrm{In}_n^{(2)}(t)),\quad n=1,\cdots,20\\ \mathrm{Out}_{21}^{(2)}(t)\equiv 1\end{cases} \tag{28}$$

where w_{ni} are the connection weights between the neurons in the input layer and hidden layer. Finally the neurons in the output layer provide the time-varying gains and burn structure parameters for Lyapunov-based guidance, the input and the output corresponding to the neurons in the output layer are given by

$$\begin{cases}\mathrm{In}_j^{(3)}(t)=\sum_{n=1}^{21}w_{jn}\cdot\mathrm{Out}_n^{(2)}(t)\\ \mathrm{Out}_j^{(3)}(t)=F(\mathrm{In}_j^{(3)}(t)),\quad j=1,2,\cdots,7\\ W_\xi(t)=\mathrm{Out}_j^{(3)}(t),\quad j=1,2,\cdots,5\\ \omega_a(t)=\mathrm{Out}_6^{(3)}(t)\\ \omega_p(t)=\mathrm{Out}_7^{(3)}(t)\end{cases} \tag{29}$$

where w_{jn} are the connection weights between the neurons in the hidden layer and output layer. Just like the minimum-time transfer, the ICEA is applied to determine the optimal weights set $\boldsymbol{\pi}^*$ for a time-fixed minimum-propellant transfer.

The optimality of a time-fixed minimum-propellant transfer should be defined with respect to the propellant consumption. When the Lyapunov-based guidance law and the periapis and apoapsis centered burn structure are used for trajectory optimization, the accuracy of the trajectory with respect to the terminal constraints must also be considered as a secondary optimization objective. For a time-fixed minimum-propellant transfer, the performance index must include the propellant consumption and the final distance to the geostationary orbit. Then, the primary sub-objective function corresponding to the propellant consumption is defined by

$$J_m=\frac{m(t_0)}{2m(t_0)-m(t_f)}-\frac{1}{3} \tag{30}$$

where m is the spacecraft mass. The total objective function for time-fixed minimum-propellant transfers is modified by

$$J=\begin{cases}-\dfrac{1}{c_4+(1-c_4)\sqrt{\left((\Delta a_f)^2+(\Delta e_f)^2+(\Delta i_f)^2\right)/3}}\\ \qquad\text{if } J_a<0, J_e<0, J_i<0\\ J_m-\dfrac{1}{c_4+(1-c_4)\sqrt{\left((\Delta a_f)^2+(\Delta e_f)^2+(\Delta i_f)^2\right)/3}}\\ \qquad\text{if } J_a\geq 0, J_e\geq 0, J_i\geq 0\end{cases} \tag{31}$$

The value for c_4 guarantees that once the requirement about terminal constraints is fulfilled, minimizing the propellant consumption has a higher priority than the improvements in the fulfillment of the terminal constraints. Here, $c_4=0.99$ is chosen.

In order to find a time-fixed minimum-propellant transfer, the proposed method runs in two loops. The particular architecture sketched in Fig. 6 reflects its fundamental design principle to search for a time-fixed minimum-propellant transfer. Within the inner loop (the trajectory integration loop), an ANN is applied to provide the time-varying gains for Lyapunov-based guidance and the burn structure parameters for equation of motion according to its network function, that is completely determined by the ANN's weight set $\boldsymbol{\pi}$, which is adjusted and evaluated by the ICEA in the outer loop(the trajectory optimization loop). Within the trajectory optimization loop, the ICEA evaluates all ANN weight sets for their suitability to generate a time-fixed minimum-propellant transfer. Within the trajectory integration loop, the ANN takes the osculating equinoctial elements $\boldsymbol{\xi}(t_i)$, the osculating satellite mass $m(t_i)$ and the target equinoctial elements $\boldsymbol{\xi}_T$ as input values and maps them to the output values, from which the time-varying gains and the burn structure parameters can be derived. The required thrust program $\hat{\boldsymbol{u}}(t_i)$ can be calculated by using the Lyapunov-based guidance. Then, the osculating equinoctial elements $\boldsymbol{\xi}(t_i)$, the osculating satellite mass $m(t_i)$ and the actual thruster program $\hat{\boldsymbol{u}}(t_i)$ are inserted into the equations of motion, which are numerically integrated over one step $\Delta t=t_{i+1}-t_i$ to yield $\mathbf{x}(t_{i+1})$. This orbit state is fed back into the ANN until the termination condition is met. After that, the ANN's weight set is evaluated by the ICEA's

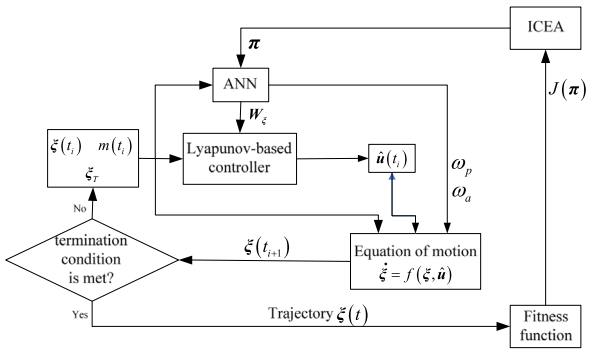

Fig. 6. The architecture of time-fixed fuel-optimal method.

fitness function $J(\boldsymbol{\pi})$, which is crucial for the probability of $\boldsymbol{\pi}$ to create optimal weight set $\boldsymbol{\pi}^*$. Finally, The ICEA converges against a single time-fixed minimum-propellant steering strategy, which adjusts the Lyapunov-based guidance to guide the spacecraft to fly along a time-fixed minimum-propellant transfer $\boldsymbol{\xi}^*[t]$.

5. Presentation of result

Results for two orbit transfer cases are presented in this section. The first case involves finding the minimum-time transfer and the time-fixed minimum-propellant transfer from a geostationary transfer orbit (GTO) to a geostationary orbit (GEO). The second case involves finding the minimum-time transfer and the time-fixed minimum-propellant transfer from a GTO to a GEO in the presence of Earth J2 perturbation and Earth-shadow eclipse effect.

5.1. GTO to GEO transfer

The assumptions given by Geffory [27] are adopted here to reproduce a transfer from a geostationary transfer orbit to a geostationary orbit. The initial mass of the spacecraft is 2000 kg, the specific impulse and the maximum thrust of the propulsion system are 2000 s and 0.35 N, respectively. The values of the gravitational constant and the gravitational acceleration in sea level are 398600.47 km^3/s^2 and 9.8665 m/s^2, respectively. The initial and final values of the Keplerian orbital elements are given in Table 1. Run-time is the time during as computed by the Fortran CPU_TIME commands. All numerical computations were performed on a PC with a 2.66 GHz processor. However, run times are not given in reference [27], and thus cannot be compared in this paper.

For the minimum-time transfer, the method was run five times with no coast arc. The maximum transfer time is set as 200 days. The threshold for the terminal errors are set to $\Delta a_{f,\max} = 36$ km, $\Delta e_{f,\max} = 8.5 \times 10^{-4}$ and $\Delta i_{f,\max} = 0.1$ deg, respectively. The best found minimum-time transfer differs by only 0.2 days, or 0.15% if compared to the reference trajectory in Ref. [27].

The final distance to the target orbit is $\Delta a_f = 8.36$ km, $\Delta e_f = 8.4 \times 10^{-4}$ and $\Delta i_f = 4.6 \times 10^{-4}$ deg, both being smaller than the required values. For the time-fixed minimum-propellant transfer, the method is used to find the optimal time-varying gains and the burn structure parameters. The transfer time is set as $t_f = 150$ days. The best found time-fixed minimum-propellant transfer gives a 4.03 kg decrease in fuel consumption if compared to the reference trajectory in Ref. [27]. The time-fixed minimum-propellant transfer gives a 23.75 kg or 11.22% decrease in fuel consumption for a 12.7 days or 9.25% increase in transfer time if compared to the minimum-time transfer. The final distance to the target orbit is $\Delta a_f = 0.0678$ km, $\Delta e_f = 3.2 \times 10^{-6}$ and $\Delta i_f = 1.8 \times 10^{-4}$ deg, both being smaller than the required values. The performances of the minimum-time transfer and the time-fixed minimum-propellant transfer are given in Table 2.The time histories of semi-major axis, eccentricity, inclination and spacecraft mass for the minimum-time transfer and the time-fixed minimum-propellant transfer are given in Fig. 7. They show good agreement with the reference trajectory. Figs. 8 and 9 present the optimal gains for the minimum-time transfer and the time-fixed minimum-propellant transfer, respectively. Fig. 10 shows the parameters for the periapis-and-apoapsis-centered burn structure, where the apogee ratio and the perigee ratio refer to w_a and w_p, respectively.

Table 1
Initial and final orbital parameters.

parameter	value	parameter	value
a_0	24505.9 km	a_f	42165 km
e_0	0.725	e_f	0
i_0	7°	i_f	0°
Ω_0	0°	Ω_f	–
ω_0	0°	ω_f	–

Table 2
Comparison of the GTO-GEO results.

	Transfer time/days	Fuel mass/kg	Fuel mass ratio/m_f/m_o
Reference [27]			
Mini-time	137.5	212	0.8940
Mini-fuel	150	192	0.9040
This paper			
Mini-time	137.3	211.72	0.8941
Mini-fuel	150	187.97	0.9060

5.2. GTO to GEO transfer with J2 perturbation and shadow effect

This case involves finding the minimum-time transfer and the time-fixed minimum-propellant transfer from a GTO to a GEO in the presence of Earth J2 perturbation and Earth-shadow eclipse effect. The assumptions given by Ref. [21] are adopted in this paper. The initial mass of spacecraft is 450 kg, the nominal power level, propulsive efficiency and specific impulse of the propulsion system are 5 kW, 65% and 3300 s, respectively. The values of the gravitational constant and the gravitational acceleration in sea level are 398574 km^3/s^2 and 9.81 m/s^2, respectively. The initial epoch required in Earth shadow computation is January 1, 2008 and the initial and final orbital elements are given in Table 3.

For the minimum-time transfer, the method was run five times with no coast arc. The maximum transfer time is set as 100 days. The threshold for the terminal errors are set to $\Delta a_{f,\max} = 36$ km, $\Delta e_{f,\max} = 8.5 \times 10^{-4}$ and $\Delta i_{f,\max} = 0.1$ deg, respectively. The best found minimum-time transfer differs by only 0.37 days, or 0.56% if compared to the reference trajectory in Ref. [21]. The terminal errors are $\Delta a_f = 3.74$ km, $\Delta e_f = 8.5 \times 10^{-4}$ and $\Delta i_f = 1.1 \times 10^{-4}$ deg, both being smaller than the required values. For the time-fixed minimum-propellant transfer, the method is used to find the optimal time-varying gains and the burn structure parameters. The transfer time is set as $t_f = 100$ days. The best found time-fixed minimum-propellant transfer is in close agreement with reference trajectory in Ref. [21]. The time-fixed minimum-propellant transfer gives a 5.35 kg or 15.33% decrease in fuel consumption for a 33.57 days or 50.53% increase in transfer time if compared to the minimum-time transfer. The terminal errors are $\Delta a_f = 7.6 \times 10^{-3}$ km, $\Delta e_f = 2.9 \times 10^{-6}$ and $\Delta i_f = 2.4 \times 10^{-3}$ deg, both being smaller than the required values. The performances of the minimum-time transfer and the time-fixed minimum-propellant transfer are given in Table 4.

The time histories of semi-major axis, eccentricity, inclination and spacecraft mass for the minimum-time transfer and the time-fixed minimum-propellant transfer are given in Fig. 11. They show good agreement with the reference trajectory. Figs. 12 and 13 present the optimal gains for the minimum-time transfer and the time-fixed minimum-propellant transfer, respectively. Fig. 14 shows the parameters for the periapis-and-apoapsis-centered burn structure, where the apogee ratio and the perigee ratio refer to w_a and w_p, respectively. Figs. 15 and 16 show the evolution of the minimum-time transfer and the time-fixed minimum-propellant transfer, respectively. The black arc and the red arc refer to thrust arc and coast arc, respectively.

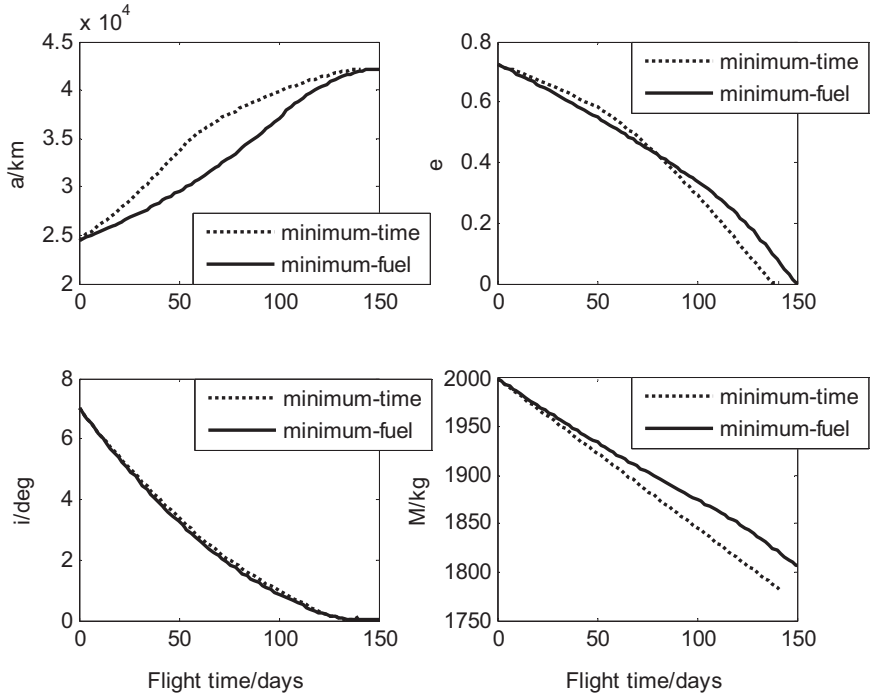

Fig. 7. The time history of Keplerian orbital elements and spacecraft mass.

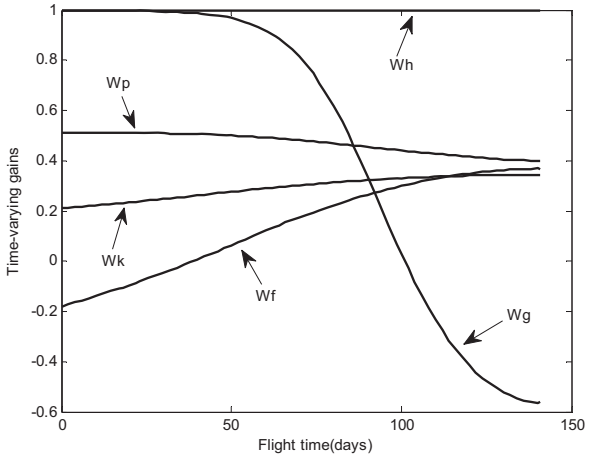

Fig. 8. The time history of gains for the minimum-time transfer.

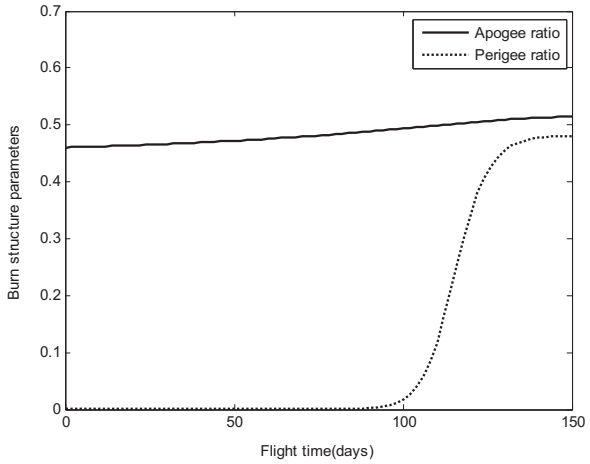

Fig. 10. The time history of the burn structure parameters.

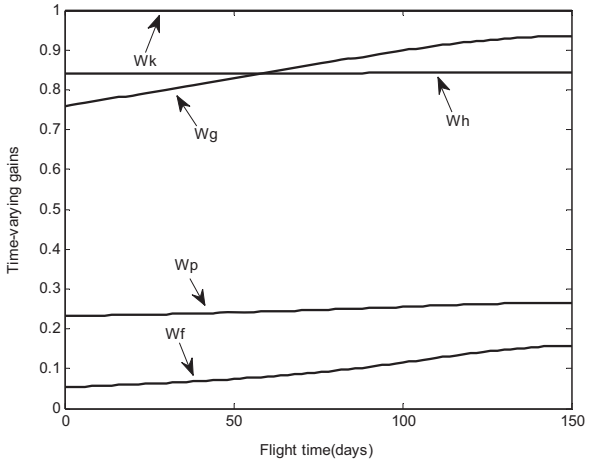

Fig. 9. The time history of gains for the time-fixed minimum-propellant transfer.

Table 3
Initial and final orbital parameters.

parameter	value	parameter	value
a_0	24364.3 km	a_f	42164 km
e_0	0.731	e_f	0
i_0	27°	i_f	0°
Ω_0	99°	Ω_f	–
ω_0	0°	ω_f	–

In this work, evolutionary algorithm (ICEA) is used as the learning algorithm for ANN, in which the search duration depends considerably on the population size of ICEA. Table 5 gives the performances of the minimum-time transfers and the search durations for several population sizes. Table 5 indicates a larger population takes longer time to converge, but the quality of the solutions does not depend considerably on the population size.

Table 4
Comparison of the GTO-GEO results.

	Transfer time/days	Fuel mass/kg	Fuel mass ratio/m_f/m_o
Reference [21]			
Mini-time	66.8	34.96	0.9223
Mini-fuel	100	29.62	0.9342
This paper			
Mini-time	66.43	34.91	0.9224
Mini-fuel	100	29.56	0.9343

6. The on-orbit autonomous flight performance

To assess the on-orbit autonomous flight performance of this Lyapunov-based guidance further, the minimum-time guidance and the time-fixed minimum-propellant guidance have been evaluated under simulated orbit determination error, random attitude error and random disturbing forces acting on the spacecraft.

The simulated orbit determination error is intended to model random errors in the measurement of the spacecraft's position and velocity. When implemented on-orbit, the orbit determination module is supposed to do real-time position estimation within 0.3 km RMS and velocity estimation within 3 m/s RMS. The simulated random attitude error is intended to model random thrust direction error. This is because the adjustment of the thrust direction is done by adjusting the satellite attitude. When implemented on-orbit, the attitude determination module is supposed to real-time attitude estimation within 0.1 deg RMS. For the only perturbation considered in this paper is the Earth J2 perturbation, the simulated disturbing forces acting on the spacecraft is intended to model other perturbations, such as luni-solar perturbations, solar radiation pressure effects and some unpredictable perturbations, that have been explicitly excluded from the simulation model. The random disturbing force is simulated by adding an additional random acceleration term to Eq. (2).

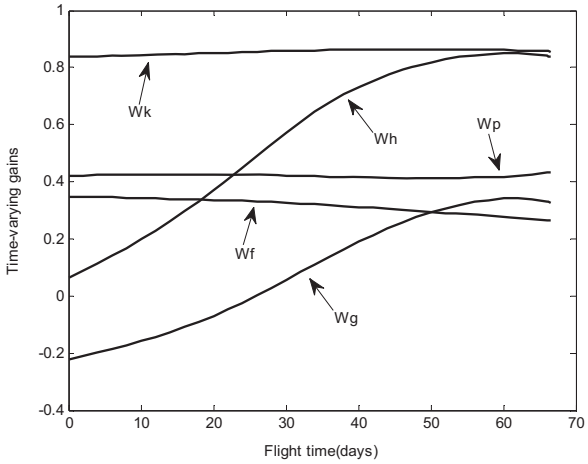

Fig. 12. The time history of gains for the minimum-time transfer.

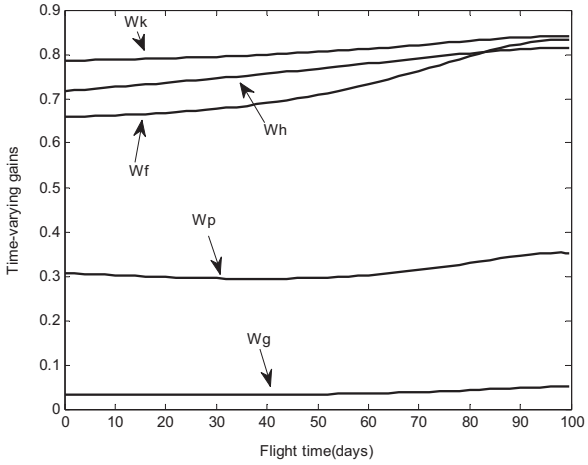

Fig. 13. The time history of gains for the time-fixed minimum-propellant transfer.

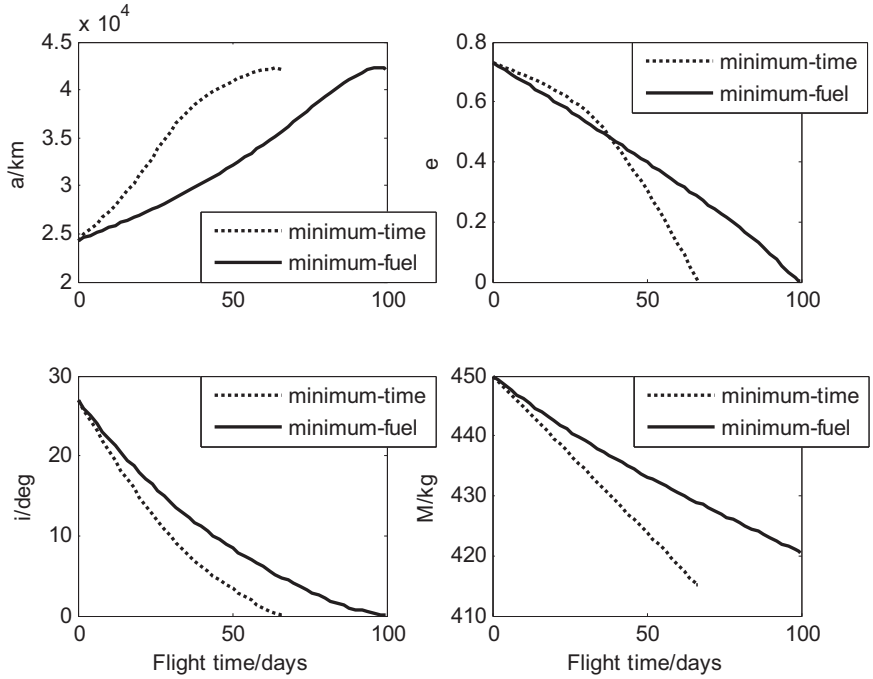

Fig. 11. The time history of Keplerian orbital elements and spacecraft mass.

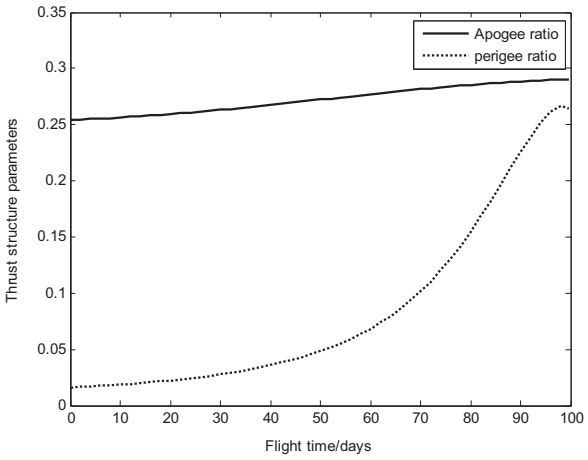

Fig. 14. The time history of the burn structure parameters.

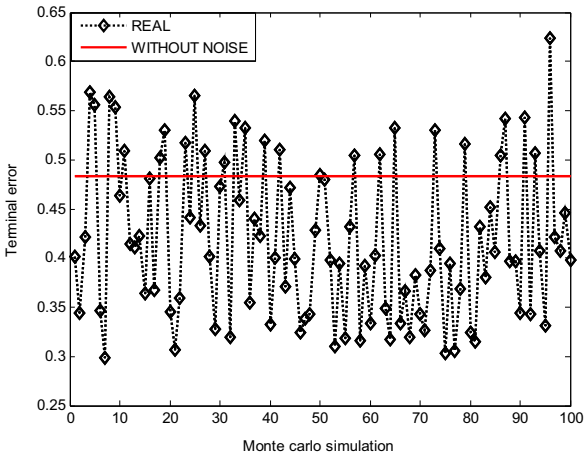

Fig. 17. The accuracy of the minimum-time guidance.

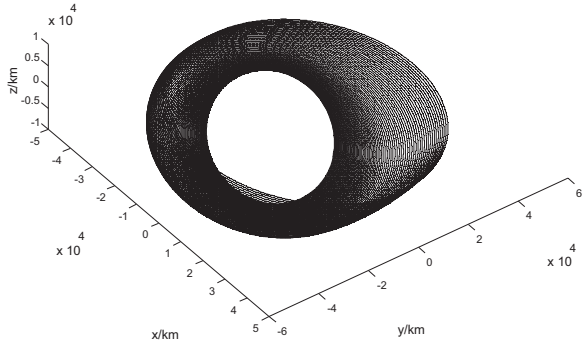

Fig. 15. The evolution of the orbit for the minimum-time transfer.

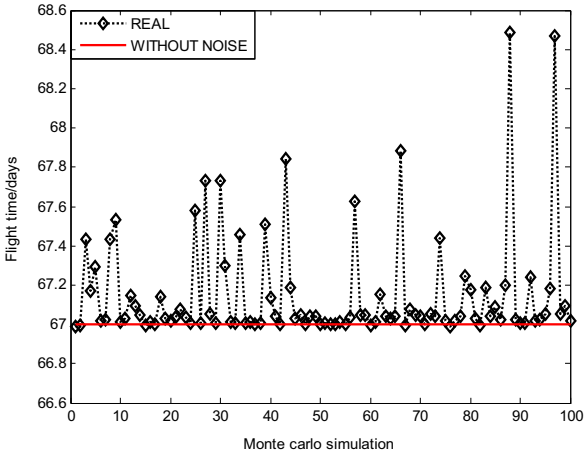

Fig. 18. The performances of the minimum-time guidance.

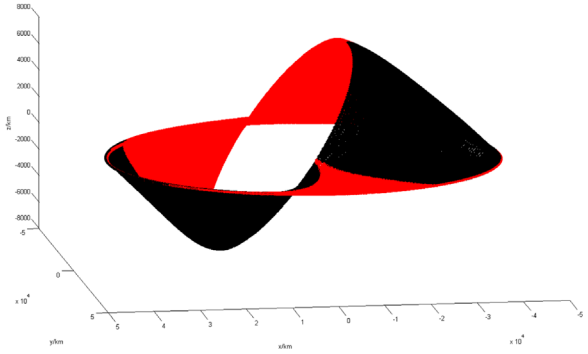

Fig. 16. The evolution of the orbit for the time-fixed minimum-propellant transfer.

Table 5
Transfer times and search durations for different population sizes.

Population size	Optimal transfer time (days)	Search duration (hours)
50	67.2	2.05
200	*66.43*	*3.2*
1000	66.76	6.8

6.1. *Minimum-time guidance*

One hundred random simulations are performed to preliminarily investigate the performance of the minimum-time guidance. Fig. 17 presents the final accuracy of the minimum-time GTO-GEO transfer under the orbit determination error, the attitude error and the model error described above. The final accuracy is a measure of distance to target that is used to determine whether the spacecraft has reached target orbit. The value of the final accuracy is less than threshold value, if the spacecraft has reached target orbit, and more than threshold value, if it is not. The detailed expression has been given in Eq. (27). Fig. 18 presents the performances (the transfer time) of the minimum-time transfers under the above error.

6.2. *Time-fixed minimum-propellant guidance*

One hundred random simulations are performed to preliminarily investigate the performance of the time-fixed minimum-propellant guidance. Fig. 19 presents the final accuracy of the time-fixed minimum-propellant GTO-GEO transfer under the orbit determination error, the attitude error and the model error described above. Fig. 20 presents the performances (the fuel consumption) of the minimum-time transfers under the above error.

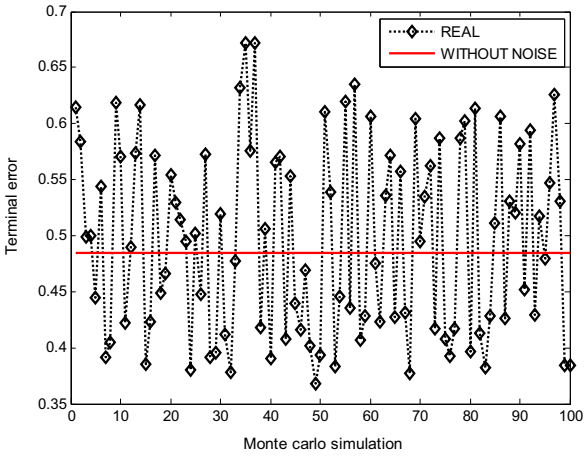

Fig. 19. The accuracy of the time-fixed minimum-propellant guidance.

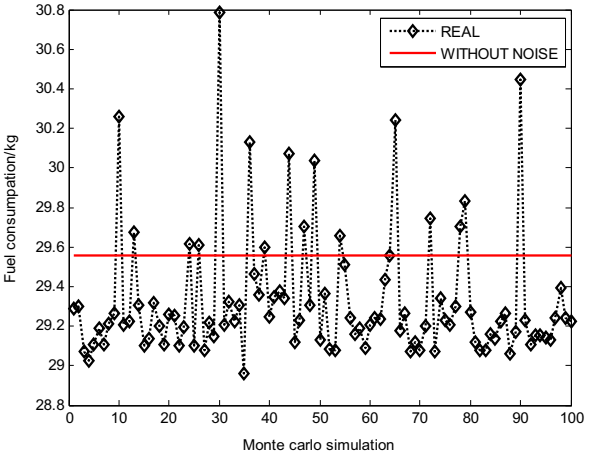

Fig. 20. The performances of the time-fixed minimum-propellant guidance.

7. Conclusion

The simulation results shown indicate clearly that the smart Lyapunov-based guidance scheme for low-thrust steering is a very promising approach for finding near globally time-optimal and time-fixed fuel-optimal low-thrust spiral trajectories. The obtained spiral trajectories are fairly accurate with respect to the terminal constraint, and the results show a satisfactory on-orbit autonomous flight performance. Therefore, the smart Lyapunov-based guidance scheme may be selected as an autonomous guidance scheme for a real space mission.

Acknowledgment

This work was carried out with financial support from the National Basic Research Program 973 of China (2013CB834103), the National Key Basic Research Program of China (2015CB857100) and the Satellite Communication and Navigation Collaborative Innovation Center (No. SatCN-201409).

References

[1] T.N. Edelbaum, Optimum power-limited orbit transfer in strong gravity fields, AIAA J. 3 (5) (1965) 921–925.
[2] D.F. Lawden, Optimal transfers between coplanar elliptical orbits, J. Guid. Control Dyn. 15 (3) (1992) 788–791.
[3] J.T. Betts, Survey of numerical methods for trajectory optimization, J. Guid. Control Dyn. 21 (2) (1998) 193–207.
[4] J.T. Betts, Very low-thrust trajectory optimization using a direct SQP method, J. Comput. Appl. Math. 120 (1) (2000) 27–40.
[5] Y. Ulybyshev, Continuous thrust orbit transfer optimization using large-scale linear programming, J. Guid. Control Dy. 30 (2) (2007) 427–436.
[6] J.A. Kechichian, Optimal low earth orbit geostationary earth orbit intermediate acceleration orbit transfer, J. Guid. Control Dyn. 20 (4) (1997) 803–811.
[7] T. Haberkorn, P. Martinon, J. Gergaud, Low thrust minimum-time orbital transfer: a homotopic approach, J. Guid. Control Dyn. 27 (6) (2004) 1046–1060.
[8] S.R. Oleson, R.M. Myars, Advanced propulsion for geostationary orbit insertion and north-south station keeping, J. Spacecr. Rockets 34 (1) (1997) 22–28.
[9] C.A. Kluever, Optimal geostationary orbit transfers using onboard chemical-electric propulsion, J. Spacecr. Rockets 49 (6) (2012) 1174–1182.
[10] Liu Tao, He Zhao-wei, Zhao Yu-shan, Continuous-thrust orbit maneuver optimization using modified robust algorithm, J. Astronaut. 29 (4) (2008) 1216–1221.
[11] C.A. Kluever, Simple guidance scheme for low-thrust orbit transfers, J. Guid. Control Dyn. 21 (6) (1998) 1015–1017.
[12] A.E. Petropoulos, Simple control laws for low-thrust orbit transfers, in: AAS/AIAA Astrodynamics Specialist Conference; 2003 Aug 3–7, Big Sky, Montana, 2003. pp. 613–630.
[13] M.R. Ilgen, Low thrust OTV guidance using Lyapunov optimal feedback control techniques, in: AAS/AIAA Astrodynamics Specialist Conference; 1993 Aug 16-19, Victoria, Canada, 1993, pp. 613–630.
[14] D.E. Chang, D.F. Chichka, J.E. Marsden, Lyapunov-based transfer between elliptic Keplerian orbits, J. Discret. Contin. Dyn. Syst. Ser. B 2 (1) (2000) 57–68.
[15] A.E. Petropoulos, Low-thrust orbit transfers using candidate Lyapunov function with a mechanism for coasting, in: AAS/AIAA Astrodynamics Specialist Conference; 2004 Aug 16-19, Providence, Rhode Island, 2004, pp. 613–630.
[16] A.E. Petropoulos, Refinements to the Q-law for low-thrust orbit transfers. in: AAS/AIAA Spaceflight Mechanics Meeting; 2005 Jan 23-27, Copper Mountain, Colorado, 2005, pp. 963–982.
[17] D.L. Yang, B. Xu, Y.T. Gao, Control method for Earth satellite orbit transfer using electric propulsion, J. Astronaut. 9 (36) (2015) 883–890.
[18] S. Lee, A.P. Von, W. Fink, et al., Comparison of multi-objective genetic algorithm in optimizing Q-law low-thrust orbit transfers. in: AAS/AIAA Spaceflight Mechanics Meeting, 2005 Jan 23–27, Copper Mountain, Colorado, 2005, pp. 613–630.
[19] Y. Ren, P.Y. Cui, E.J. Luan, A low-thrust guidance law based on Lyapunov feedback control and hybrid genetic algorithm, Aircr. Eng. Aerosp. Technol. 79 (2) (2007) 144–149.
[20] Y. Gao, Direct optimization of low-thrust many-revolution earth-orbit transfers, Chin. J. Aeronaut. 22 (4) (2009) 426–433.
[21] Y. Gao, X. Li, Optimization of low thrust many revolution transfers and Lyapunov based guidance, Acta Astronaut. 66 (1) (2010) 117–129.
[22] D.L. Yang, B. Xu, Y.T. Gao, Optimal strategy for low-thrust spiral trajectories using Lyapunov-based guidance, Adv. Space Res. 56 (5) (2015) 865–878.
[23] J. Walker, B. Ireland, J. Owens, A set of modified equinoctial elements, Celest. Mech. 36 (4) (1985) 409–419.
[24] L. Sackett, H.L. Malchow, T.N. Edelbaum, Solar electric geocentric transfer with attitude constraints: analysis. NASA CR-134927, Aug, 1975, pp. 112–138.
[25] R. Rojas, Neutral Network: A Systematic Introduction, Springer, Berlin, Heidelberg: New York, 1996.
[26] H. Lei, B. Xu, Y. Sun, Earth-moon low energy trajectory optimization in the real system, Adv. Space Res. 51 (5) (2013) 917–929.
[27] S. Geffory, R. Epenoy, Optimal low-thrust transfers with constraints-generalization of averaging techniques, Acta Astonaut. 41 (3) (1997) 133–149.